

See discussions, stats, and author profiles for this publication at: <https://www.researchgate.net/publication/239721785>

Density Functional Calculation of $^1J_{C-H}$ Coupling Constants in Cyclohexane and Diheterocyclohexanes. Repercussion of Stereoelectronic Effects on Coupling Constants

ARTICLE in THE JOURNAL OF PHYSICAL CHEMISTRY A · FEBRUARY 1999

Impact Factor: 2.69 · DOI: 10.1021/jp983664s

CITATIONS

64

READS

25

3 AUTHORS, INCLUDING:



Alberto Vela

Center for Research and Advanced Studies of...

126 PUBLICATIONS 2,519 CITATIONS

SEE PROFILE

Density Functional Calculation of $^1J_{\text{C-H}}$ Coupling Constants in Cyclohexane and Diheterocyclohexanes. Repercussion of Stereoelectronic Effects on Coupling Constants

Gabriel Cuevas,^{*,1} Eusebio Juaristi,^{*,2} and Alberto Vela^{*,2,3}

Instituto de Química, Universidad Nacional Autónoma de México, Cd. Universitaria, Apdo. Postal 70213, 04510 Coyoacán México, D.F., México, Departamento de Química, Centro de Investigación y de Estudios Avanzados del Instituto Politécnico Nacional, Apdo. Postal 14-740, 07000 México, D.F., México, and Departamento de Química, División de Ciencias Básicas e Ingeniería, Universidad Autónoma Metropolitana Iztapalapa, Apdo. Postal 55534, 09340 México, D.F., México

Received: September 21, 1998

Ab initio calculations, within the framework of density functional theory, were carried out on cyclohexane, 1,3-dioxane, 1,3-dithiane, 1,3-oxathiane, and 1,3-diazane. The one-bond ^{13}C – ^1H NMR coupling constants were estimated according to the recently proposed theory by Malkin, Malkina, and Salahub. [Malkin, V. G.; Malkina, O. L.; Salahub, D. R. *Chem. Phys. Lett.* **1994**, 221, 91]. No correlation between one-bond ^{13}C – ^1H spin–spin coupling constants and the corresponding C–H bond distances was found. The direction of the Perlman effect, defined as the difference between the axial minus the equatorial one-bond C–H coupling constants, is correctly predicted by this methodology for all cases with the exception of one methylene group in 1,3-oxathiane. Thus, in general, the methodology is capable of reproducing subtle properties that are driven by stereoelectronic interactions.

Introduction

Forty years ago, Bohlmann noticed that C–H bonds anti-periplanar (app) to a vicinal nitrogen lone pair in conformationally defined amines give rise to characteristic infrared stretching frequencies (“Bohlmann bands”),⁴ presumably as a result of $n_{\text{N}} \rightarrow \sigma^*_{\text{C-H}_{\text{app}}}$ hyperconjugation⁵ (Scheme 1).

Similar stereoelectronic interaction may be responsible for the significant difference in one-bond ^{13}C – ^1H ($^1J_{\text{C-H}}$) coupling constants presented by methylenic C–H bonds adjacent to oxygen or nitrogen in a six-membered ring. Specifically, at the anomeric position of tetrahydropyrans, the axial C–H bond coupling constant is generally smaller by 8–10 Hz than $^1J_{\text{C-H}_{\text{eq}}}$, that is, $^1J_{\text{C-H}_{\text{ax}}} < ^1J_{\text{C-H}_{\text{eq}}}$ (“Perlman effect”).^{6,7}

Interestingly, whereas *cis*-4,6-dimethyl-1,3-dioxane (**1**, Chart 1) presents a normal Perlman effect at C(2): $^1J_{\text{C-H}_{\text{ax}}} = 157.4 \text{ Hz} < ^1J_{\text{C-H}_{\text{eq}}} = 167.5 \text{ Hz}$,^{7a} the dithiane analogue **2** (Chart 1) exhibits a “reverse Perlman effect”: $^1J_{\text{C(2)-H}_{\text{ax}}} = 154.1 \text{ Hz} > ^1J_{\text{C(2)-H}_{\text{eq}}} = 144.9 \text{ Hz}$.⁸

The observed reversal of the relative magnitudes of the coupling constants at C(2) in dioxane and dithiane parallels the opposite trends in C–H bond lengths estimated for C(2)–H in these heterocycles: the axial C–H bond is longer in dioxane, but the equatorial one is longer in dithiane,⁹ and this may be the result of dominant $\sigma_{\text{C-S}} \rightarrow \sigma^*_{\text{C-H}_{\text{eq}}}$ (rather than $n_{\text{S}} \rightarrow \sigma^*_{\text{C-H}_{\text{ax}}}$) interactions in **2**.^{9–11}

In this context, *ab initio* Hartree–Fock 6-31G(*d,p*) calculations on 1,3-dioxane and 1,3-dithiane¹¹ seem to support arguments based on stereoelectronic ($n_{\text{O}} \rightarrow \sigma^*_{\text{C-H}_{\text{ax}}}$ and $\sigma_{\text{C-X}} \rightarrow \sigma^*_{\text{C-H}_{\text{eq}}}$) interactions as responsible for the anomalous situation pointed out by Eliel and co-workers,¹² where contrary to the normal case in which axial protons in a cyclohexane ring resonate upfield of the corresponding equatorial ones, in 1,3-dithiane H(2_{ax}) is downfield from H(2_{eq}), whereas in 1,3-dioxane H(5_{ax}) is downfield from H(5_{eq}).

SCHEME 1

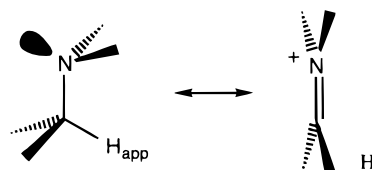
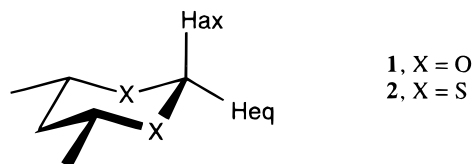


CHART 1



Motivated by the successful application of the density functional calculation of ^1H NMR chemical shifts for cyclohexane, 1,3-dioxane, 1,3-dithiane, and 1,3-oxathiane,¹³ this work reports density functional theory calculations¹⁴ of one-bond ^{13}C – ^1H coupling constants in cyclohexane and 1,3-diheterocyclohexanes. Not only are *ab initio* calculations of coupling constants scarce,¹⁵ but also, the potential manifestation of stereoelectronic effects in these heterocycles, as discussed above, introduces an additional complicating factor to test available methods for the calculation of coupling constants.

Computational Methods

Full geometry optimizations (no symmetry constraints) of cyclohexane, 1,3-dioxane, 1,3-dithiane, and 1,3-oxathiane were carried out using density functional theory (DFT). The semilocal (generalized gradient corrected) exchange–correlation energy functional used was that with the exchange functional of Becke¹⁶ and the correlation energy functional of Perdew (BP).¹⁷ The semilocal corrections are incorporated self-consistently. The

orbital basis set was a double- ζ plus polarization (DZVP2), and the auxiliary basis set to fit the charge density and the exchange-correlation potential was A1, in the deMon or Dgauss notation. For the numerical integration a FINE grid was selected. These geometry optimizations were done using the Dgauss 1.1 program.¹⁸

Complete geometry optimizations (without symmetry constraints) of three different N–H arrangements of 1,3-diazane were performed using the hybrid functional B3LYP with a 6-31G(d,p) basis set. These calculations were done with the Gaussian 92 Program (G92).¹⁹ As is well-known,²⁰ in this functional, the exchange is combined with a local and gradient-corrected correlation functional. The correlation functional used is actually $C^*E_C^{\text{LYP}} + (1 - C^*)E_C^{\text{VWN}}$, where LYP is the correlation functional of Lee, Yang, and Parr,²¹ which includes both local and gradient corrected terms, and VWN is the Vosko, Wilk, and Nusair 1980 correlation functional fitting the RPA solution to the uniform gas, often referred to as local spin density (LSD) correlation.²² VWN is used to provide the excess local correlation required, since LYP contains a local term essentially equivalent to VWN.²¹

The density functional calculation of ^1H and ^{13}C coupling constants was done using the recent approach proposed by Malkin, Malkina, and Salahub.^{14b,23,24} Within this methodology, three contributions to the NMR spin–spin coupling constants are considered, namely, the Fermi contact (FC), the paramagnetic spin–orbit (PSO) and the diamagnetic spin–orbit (DSO). The spin-dipolar (SD) and cross terms such as FC–SD are neglected. The FC term is calculated by finite perturbation theory (FPT), the PSO contribution is obtained using the sum-over-states density functional perturbation theory (SOS-DFPT),^{14a} and the DSO term is obtained by numerical integration.^{23,24} These spin–spin coupling constants calculations were done with a modified version of the deMon-KS program^{25,26} together with the deMon-NMR program.^{23,24,25} Following the suggestions made by the authors of this latter code, the NMR spin–spin coupling constants were calculated using the semilocal exchange of Perdew and Wang²⁷ and the correlation functional of Perdew,²⁸ a combination that will be denoted as PP. A value of 0.001 was used for the perturbation parameter in the FPT calculation of the FC term and the lighter nucleus is selected as the perturbation center. The PSO contribution was obtained with the Local 1 approximation.¹⁴ A fine grid (with 32 radial points) with an extra iteration was used, and the basis set employed in the coupling constants calculations was the IGLO-III of Kutzelnigg.²⁹

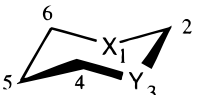
The natural bond orbital (NBO) analysis of 1,3-diazane was carried out with the 3.1 NBO program as implemented in G92.³⁰

To compare the effect of geometry in the calculation of coupling constants for cyclohexane, 1,3-dioxane, 1,3-dithiane, and 1,3-oxathiane, three sets of fully optimized geometries were tested: (1) those obtained by Dgauss using the BP exchange-correlation functional (BP/DZVP2), (2) the geometry provided by deMon-KS with the PP exchange-correlation functional (PP/DZVP2), and (3) those obtained using the hybrid functional B3LYP with G92. Thus, following the usual notation, three sets of coupling constants are reported in this work, namely, PP/IGLO-III//BP/DZVP2, PP/IGLO-III//PP/DZVP2 and PP/IGLO-III//B3LYP/6-31G(d,p). For 1,3-diazanes, coupling constants were determined with PP/IGLO-III//B3LYP/6-31G(d,p).

Results and Discussion

The structure of cyclohexane (3, Table 1), calculated by ab initio DFT BP/DZVP2 and PP/DZVP2 methods, has recently

TABLE 1: Optimized Geometries (Distances in Å, angles in deg) for 1,3-Dioxane (4), 1,3-Dithiane (5), and 1,3-Oxathiane (6)



3, X = Y = CH₂
 4, X = Y = O
 5, X = Y = S
 6, X = O, Y = S

	4	5	6
X–C ₂	1.407	1.830	1.402
C ₂ –Y			1.845
Y–C ₄	1.427	1.838	1.841
C ₄ –C ₅	1.531	1.533	1.532
C ₅ –C ₆			1.532
C ₆ –X			1.425
C ₂ –H _{ax}	1.108	1.094	1.101
C ₂ –H _{eq}	1.091	1.092	1.091
C ₄ –H _{ax}	1.104	1.097	1.097
C ₄ –H _{eq}	1.093	1.093	1.093
C ₅ –H _{ax}	1.095	1.095	1.095
C ₅ –H _{eq}	1.097	1.099	1.098
C ₆ –H _{ax}			1.104
C ₆ –H _{eq}			1.093
X–C ₂ –Y	113.2	115.6	113.8
C ₂ –Y–C ₄	11.0	98.5	95.4
Y–C ₄ –C ₅	110.3	114.4	111.3
C ₄ –C ₅ –C ₆	108.7	114.0	112.4
C ₅ –C ₆ –X			112.9
C ₆ –X–C ₂			112.9
X–C ₂ –Y–C ₄	60.9	59.5	55.8
C ₂ –Y–C ₄ –C ₅	56.4	57.8	50.6
Y–C ₄ –C ₅ –C ₆	52.7	65.9	57.9
C ₄ –C ₅ –C ₆ –X			60.6
C ₅ –C ₆ –X–C ₂			64.8
C ₆ –X–C ₂ –Y			66.8
H _{ax} –C ₂ –Y–C ₄	61.7	65.0	67.9
H _{eq} –C ₂ –Y–C ₄	178.7	178.0	174.4
H _{ax} –C ₄ –Y–C ₂	64.9	66.5	72.0
H _{eq} –C ₄ –Y–C ₂	178.3	178.9	172.1
H _{ax} –C ₅ –C ₄ –Y	66.5	57.7	63.5
H _{eq} –C ₅ –C ₄ –Y	174.4	174.5	178.6
H _{ax} –C ₆ –X–C ₂			58.1
H _{eq} –C ₆ –X–C ₂			174.1

been reported.¹³ Table 1 collects the structural data for 1,3-dioxane (4), 1,3-dithiane (5), and 1,3-oxathiane (6) calculated at the B3LYP/6-31G(d,p) level of theory. These data agree quite well with those obtained at BP/DZVP2 and PP/DZVP2 levels of theory.¹³

Table 2 presents the experimental and calculated $^1J_{\text{C-H}}$ coupling constants for cyclohexane (3). It is appreciated that the calculations reproduce the relative magnitude of both the C–H_{ax} and C–H_{eq} coupling constants, that is, the normal Perlin effect observed in cyclohexane,³¹ as well as the absolute values, within reasonable limits (± 2 –3 Hz).

The experimental and calculated one-bond ^{13}C – ^1H coupling constants for 1,3-dioxane (4) are presented in Table 2. The relative magnitudes of the calculated average coupling constants for C(2) (158.8 Hz), C(4,6) (138.5 Hz), and C(5) (125.0 Hz) are in line with the decreasing inductive effect by two, one, and zero adjacent oxygen atoms at these positions. Furthermore, calculation reproduces the Perlin effect that is experimentally found at C(2) in 1,3-dioxane, i.e., $^1J_{\text{C-H}_{\text{ax}}} < ^1J_{\text{C-H}_{\text{eq}}}$, that has been rationalized in terms of $n_{\text{O}} \rightarrow \sigma^*_{\text{C-H}_{\text{ax}}}$ orbital interactions.^{9–11}

At C(5) in 1,3-dioxane, $^1J_{\text{C-H}_{\text{ax}}} \cong ^1J_{\text{C-H}_{\text{eq}}}$,^{7a,11} and this experimental observation has been explained in terms of a competition between the normal Perlin effect, which weakens

TABLE 2: Experimental and Calculated One-Bond Coupling Constants in Cyclohexane (3), 1,3-Dioxane (4), 1,3-Dithiane (5), and 1,3-Oxathiane (6) (All Quantities in Hz)

compd	bond	exptl ^{11,28}	calcd ^a	calcd ^b	calcd ^c
3	C–H _{ax}	122.4	119.45	120.46	
3	C–H _{eq}	126.4	124.16	124.11	
4	C(2)–H _{ax}	158.6	152.8	152.8	147.7
4	C(2)–H _{eq}	167.5	167.6	167.4	164.5
4	C(4,6)–H _{ax}	143.6	132.5	133.1	130.3
4	C(4,6)–H _{eq}	145.0	145.0	146.3	144.0
4	C(5)–H _{ax}	128.9	128.3	129.2	127.0
4	C(5)–H _{eq}	128.9	122.0	122.3	121.4
5	C(2)–H _{ax}	154.2	150.7	150.5	150.0
5	C(2)–H _{eq}	146.2	141.9	144.6	140.7
5	C(4,6)–H _{ax}	137.3	133.8	134.4	132.8
5	C(4,6)–H _{eq}	132.9	134.4	135.1	133.0
5	C(5)–H _{ax}	130.2	129.8	128.6	127.9
5	C(5)–H _{eq}	127.4	121.0	120.8	119.6
6	C(2)–H _{ax}	157.5	152.9	153.4	150.3
6	C(2)–H _{eq}	157.5	154.4	156.8	152.9
6	C(4)–H _{ax}	142.7	133.9	133.2	132.5
6	C(4)–H _{eq}	142.7	136.7	137.0	132.5
6	C(5)–H _{ax}	126.9	129.3	128.9	127.1
6	C(5)–H _{eq}	129.0	121.1	121.7	120.1
6	C(6)–H _{ax}	139.0	132.4	133.6	130.3
6	C(6)–H _{eq}	145.0	143.9	144.1	142.2

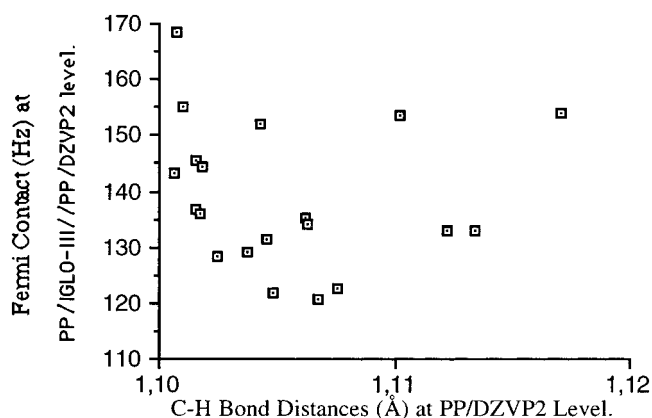
^a PP/IGLO-III//BP/DZVP2. ^b PP/IGLO-III//PP/DZVP2. ^c PP/IGLO-III//B3LYP/6-31G(d,p).

CHART 2

the axial C(5)–H bond, and a “reverse” Perlin effect that weakens the equatorial C(5)–H bond. Anderson et al.³² have suggested a stereoelectronic interaction between a pseudoequatorial nonbonding electron pair on a β -oxygen and the equatorial C–H bond (Chart 2) as responsible for the weakening of this bond. Alternatively, $\sigma_{C-O} \rightarrow \sigma^*_{C-H_{eq}}$ hyperconjugation may account for the results.¹¹

The calculated $^1J_{C(5)-H_{ax}} = 127.0\text{--}129.2$ Hz (Table 2) agrees almost perfectly with the experimentally observed value, 128.9 Hz. The weakening of the equatorial C(5)–H bond discussed in the previous paragraph is apparently reproduced by the calculations, $^1J_{C(5)-H_{eq}} = 121.4\text{--}122.3$ Hz. Nevertheless, comparison with the experimental value (128.9 Hz) shows an overemphasis in such an effect, so that a significant “reverse” Perlin effect is predicted.

Table 2 summarizes the experimental and calculated one-bond $^{13}\text{C}\text{--}^1\text{H}$ coupling constants for 1,3-dithiane (5). All calculations correctly predict the “reverse” Perlin effects at C(2) and C(5), that is, $^1J_{C-H_{ax}} > ^1J_{C-H_{eq}}$ at these methylenes. By contrast, quite similar coupling constants are calculated at C(4,6): $^1J_{C-H_{ax}} = 132.8\text{--}134.4$ Hz \approx $^1J_{C-H_{eq}} = 133.0\text{--}135.1$ Hz, whereas a “reverse” Perlin effect is found experimentally: $^1J_{C(5)-H_{ax}} = 137.3$ Hz $>$ $^1J_{C(5)-H_{eq}} = 132.9$ Hz. Considering the size and quality of the basis sets used for the calculation of the coupling constants, one should not expect that these differences in the coupling constants are due to basis set effects. Evidently, there is a problem here, perhaps associated with differences between experimental (condensed phase) and theoretical (gas phase, 0 K) geometries, although, as indicated above, no such difficulty is encountered in the calculation at C(2). As can be seen in Table 3, the contribution responsible for these differences is the FC term. The diamagnetic and paramagnetic spin–orbit contributions are much smaller than the FC term

**Figure 1.** No correlation between C–H coupling constants and corresponding optimized bond distances.**TABLE 3: Contributions to One-Bond $^{13}\text{C}\text{--}^1\text{H}$ Coupling Constants (Hz) in 1,3-Dithiane at the PP/IGLO-III//BP/DZVP2 Level of Theory**

bond	FC	PSO	DSO
C(2)–H _{ax}	149.59	0.08	1.03
C(2)–H _{eq}	140.71	0.16	0.98
C(4,6)–H _{ax}	132.47	0.38	0.96
C(4,6)–H _{eq}	133.06	0.44	0.91
C(5)–H _{ax}	128.27	0.54	0.93
C(5)–H _{eq}	119.26	0.88	0.87

and their contribution to the differences $^1J_{C-H_{ax}} - ^1J_{C-H_{eq}}$ are, at most, 1 order of magnitude smaller than the corresponding FC differences. A similar situation was obtained for the other molecules considered in this work.

Table 2 presents the experimental and calculated one-bond $^{13}\text{C}\text{--}^1\text{H}$ coupling constants for 1,3-oxathiane (6). Experimentally,¹¹ similar coupling constants $^1J_{C-H_{ax}} \approx ^1J_{C-H_{eq}}$ are observed at C(2), C(4), and C(5), suggesting a balance of the effect(s) responsible for a normal Perlin effect ($^1J_{C-H_{ax}} < ^1J_{C-H_{eq}}$), as found for C–H bonds in cyclohexane³¹ or adjacent to oxygen.^{6,7} A reverse trend is observed (i.e., $^1J_{C-H_{eq}} < ^1J_{C-H_{ax}}$) when the C–H_{eq} is antiperiplanar to C–S bonds.^{10,11} Computationally, similar coupling constants ($\Delta J < 3$ Hz) are also calculated for the axial and equatorial C–H bonds at C(2) and C(4), although a strong “reverse” Perlin effect is predicted at C(5), contrary to experiment. On the other hand, a substantial, normal Perlin effect is calculated for C(6), in line with the experimental observations.

It is worth noting that the calculations reported here show the danger of trying to correlate bond distances with coupling constants. To illustrate this, the C(2)–H_{eq} and C(2)–H_{ax} distances in 1,3-dioxane differ by 0.016 Å and the corresponding difference in coupling constants is 15 Hz, while in 1,3-dithiane, the same bond distances differ by 0.003 Å, but the difference in coupling constants is 9 Hz. Thus, at least for these molecules, it is impossible to find a linear correlation between bond distances and coupling constants. To clarify this point further, in Figure 1 the calculated $^1J_{C-H}$ coupling constants obtained in this work are plotted against their corresponding PP/DZVP2 optimized bond distances. The scattering of points prevents one from establishing the existence of any reasonable trend.

Table 4 summarizes the results presented in this section. The first feature to be noticed is that, even though the coupling constant differences change with the optimized geometry, the nature of the Perlin effect (normal or reverse) is preserved, even when the exchange–correlation functionals used to optimize the geometries belong to different classes (GGA vs hybrid). In this respect, the perfect match provided by the B3LYP optimized geometry in C(4)–H of 6 should be considered fortuitous.

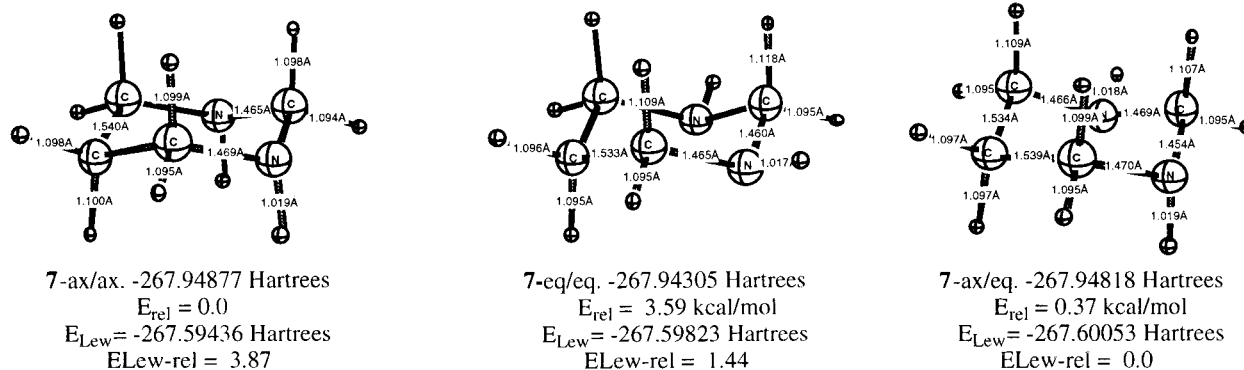


Figure 2. Structure and energy of isomeric 1,3-diazanes (7), including energies of the corresponding structures with localized electrons (E_{Lew}).

TABLE 4: Difference (in Hz) between Axial and Equatorial One-Bond ^{13}C – ^1H Coupling Constants as a Function of the Optimized Geometry^a

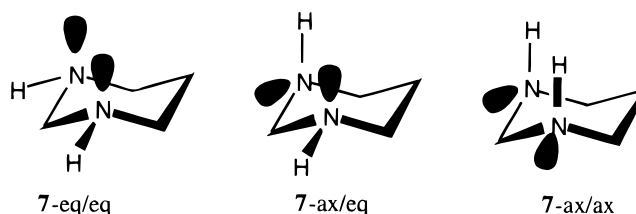
compd	bond	exptl ¹¹	BP ^b	PP ^c	B3LYP ^d
3	C–H	–4.0	–4.7	–3.6	
4	C(2)–H	–8.9	–14.8	–14.6	–16.8
4	C(4,6)–H	–1.4	–12.5	–13.2	–13.7
4	C(5)–H	0.0	6.3	6.9	5.6
5	C(2)–H	8.0	+8.8	5.9	9.3
5	C(4,6)–H	4.4	–0.6	–0.7	–0.2
5	C(5)–H	2.5	+8.8	7.8	8.3
6	C(2)–H	0.0	–1.5	–3.4	–2.5
6	C(4)–H	0.0	–2.8	–3.8	0.0
6	C(5)–H	–2.1	+8.2	7.2	7.0
6	C(6)–H	–6.0	–11.5	–10.5	–11.9

^a Negative values indicate a normal Perlin effect. ^b PP/IGLO-III/BP/DZVP2. ^c PP/IGLO-III/PP/DZVP2. ^d PP/IGLO-III/B3LYP/6-31G(d,p).

Neglecting those cases where experiment predicts no Perlin effect (C5 in 4, C2 and C4 in 6), DFT correctly predicts the observed direction of the Perlin effect, except for C(4,6) in 5 and C(5) in 6. Considering that the average absolute deviation obtained by Malkin, Malkina, and Salahub^{14b} for the $^1J_{\text{C-H}}$ constants in 21 organic molecules is of 3.5 Hz, with a greater tendency to underestimate these values (14 molecules), one can expect that the discrepancy in 1,3-dithiane can be fixed by enlarging the grid and the basis set. However, the approximately 10 Hz difference in C(5) of 6 points toward another physical effect. Solvent and thermal effects are certainly good candidates. Using the same argumentation, one can establish that if the DFT calculated $|\Delta J|$ is less than 3 Hz, by thermal averaging, the Perlin effect could vanish or be inverted. Notice that the $|\Delta J|$ DFT values at the carbon atoms where experiment establishes that there is no Perlin effect, are within the range mentioned above, except for C(5) in 1,3-dioxane. Thus, one is led to conclude that, after taking into account the errors in the DFT calculated coupling constants, this methodology is clearly capable of predicting the nature of the Perlin effect in 1,3-diheterocyclohexanes.

1,3-Diazane (7). This nitrogen analogue of heterocycles 4–6 is particularly suitable for study since axial C–H bonds adjacent to nitrogen, which are at least partly antiperiplanar (app) to the lone pair at nitrogen, are markedly longer and weaker than the corresponding equatorial ones³³ and thus are anticipated to present smaller coupling constants.^{11,34} Furthermore, stereo-electronic $\sigma_{\text{C-N}} \rightarrow \sigma_{\text{C-H}_{\text{eq}}}$ or perhaps W-array hyperconjugation with the β -nitrogen lone pair³² is predicted to provoke a “reverse” Perlin effect at C(5) in 1,3-diazane. This so-called β_{N} Wn hyperconjugative interaction should be most effective when both lone pairs are equatorial, as in 7-ax/ax (Chart 3).

CHART 3



SCHEME 2

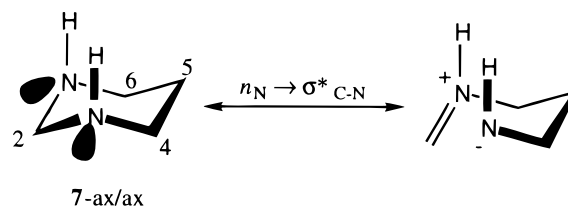


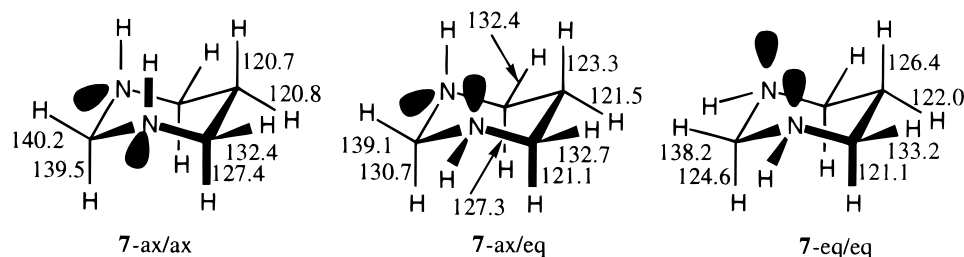
Figure 2 summarizes the relevant bond lengths (Å) in the B3LYP/6-31G(d,p) optimized structures and the calculated energies. It is estimated that 7-ax/ax and 7-ax/eq are isoenergetic. Comparison with the corresponding energies in hypothetical structures with strictly localized electrons [modeled by means of Natural Bond Orbital analysis (NBO)³⁰] suggests that $n_{\text{N}} \rightarrow \sigma^*_{\text{C-N}}$ orbital interactions stabilize these isomers. The higher energy of 7-eq/eq arises from the electronic repulsion between the 1,3-diaxial lone pairs, whereas in 7-ax/ax two $n_{\text{N}} \rightarrow \sigma^*_{\text{C-N}}$ stabilizing interactions are possible at the cost of H/H steric repulsion. (Scheme 2).

Some support for the hyperconjugative interaction depicted in Scheme 2 is gained from the structural data presented in Figure 2 and Table 5. In particular, the calculated N(1)–C(2) bond lengths decrease and the N(1)–C(2)–N(3) bond angles increase in the series 7-eq/eq (1.469 Å and 108.8°) to 7-ax/ax (1.465 Å and 117.2°) to 7-ax/eq (1.454 Å and 112.1°). These trends are consistent with the proposed $n_{\text{N}} \rightarrow \sigma^*_{\text{C-N}}$ orbital interaction.

Chart 4 presents the calculated one-bond ^{13}C – ^1H coupling constants for isomeric diazanes 7-ax/ax, 7-ax/eq, and 7-eq/eq. As expected in terms of $n_{\text{N}} \rightarrow \sigma^*_{\text{C-H}_{\text{app}}}$ hyperconjugation,³³ the axial C(2)–H bonds in 7-eq/eq and 7-ax/eq (which is at least partly app to a lone pair at nitrogen) present smaller $^1J_{\text{C-H}}$ coupling constants than the corresponding C(2)–H_{eq}. Interestingly, $^1J_{\text{C(2)-H}_{\text{ax}}} \cong ^1J_{\text{C(2)-H}_{\text{eq}}}$ in 7-ax/ax, where the nitrogen lone pair is gauche to both C–H bonds. Normal Perlin effects ($^1J_{\text{C-H}_{\text{ax}}} < ^1J_{\text{C-H}_{\text{eq}}}$) are also found at C(4,6), with $\Delta J_{\text{ax/eq}}$ being largest in 7-eq/eq.

On the other hand, β_{N} Wn hyperconjugative interactions as proposed by Anderson et al.³² should be most efficient in 7-ax/

CHART 4

**TABLE 5: Calculated Geometry (Distances in Å, Angles in deg) for Isomeric 1,3-Diazanes 7-ax/ax, 7-ax/eq, and 7-eq/eq (Chart 3) at the B3LYP/6-31G(d,p) Level of Theory**

	7-ax/ax	7-ax/eq	7-eq/eq
N ₁ —C ₂	1.465	1.469	1.460
C ₂ —N ₃		1.454	
N ₃ —C ₄	1.469	1.470	1.465
C ₄ —C ₅	1.540	1.539	1.533
C ₅ —C ₆		1.534	
C ₆ —N ₁		1.466	
N ₁ —H	1.019	1.018	1.017
C ₂ —H _{ax}	1.098	1.107	1.118
C ₂ —H _{eq}	1.094	1.095	1.095
N ₃ —H		1.019	
C ₄ —H _{ax}	1.099	1.100	1.109
C ₄ —H _{eq}	1.095	1.095	1.095
C ₅ —H _{ax}	1.100	1.097	1.095
C ₅ —H _{eq}	1.098	1.097	1.096
C ₆ —H _{ax}		1.109	
C ₆ —H _{eq}		1.096	
N ₁ —C ₂ —N ₃	117.2	112.1	108.8
C ₂ —N ₃ —C ₄	111.2	110.8	113.3
N ₃ —C ₄ —C ₅	113.4	113.3	108.8
C ₄ —C ₅ —C ₆	109.7	109.9	109.8
C ₅ —C ₆ —N ₁		108.9	
C ₆ —N ₁ —C ₂		111.0	
N ₁ —C ₂ —N ₃ —C ₄	51.4	56.5	62.6
C ₂ —N ₃ —C ₄ —C ₅	50.7	51.6	59.4
N ₃ —C ₄ —C ₅ —C ₆	51.3	50.8	55.3
C ₄ —C ₅ —C ₆ —N ₁		53.8	
C ₅ —C ₆ —N ₁ —C ₂		59.9	
C ₆ —N ₁ —C ₂ —N ₃		62.3	
H—N ₁ —C ₂ —N ₃	68.8	175.7	175.8
H—N ₃ —C ₄ —N ₁		61.9	
H _{ax} —C ₂ —N ₃ —C ₄	69.0	66.9	60.5
H _{eq} —C ₂ —N ₃ —C ₄	175.0	176.9	179.0
H _{ax} —C ₄ —N ₃ —C ₂	69.9	69.3	61.1
H _{eq} —C ₄ —N ₃ —C ₂	175.0	175.6	179.9
H _{ax} —C ₅ —C ₄ —N ₃	68.7	68.7	64.2
H _{eq} —C ₅ —C ₄ —N ₃	173.7	172.9	176.9
H _{ax} —C ₆ —N ₁ —C ₂		60.7	
H _{eq} —C ₆ —N ₁ —C ₂		179.3	

ax (equatorial lone pairs at nitrogen), so that C(5)—H_{eq} could be anticipated as longest and weakest. The calculated C(5)—H_{eq} bond distances (Table 5) are in agreement with this argument: 1.098 Å for 7-ax/ax, 1.097 Å for 7-ax/eq, and 1.096 Å for 7-eq/eq. Curiously, the C(5)—H_{ax} bond lengths are predicted to diminish even more rapidly along the series: 1.100 Å in 7-ax/ax, 1.097 Å in 7-ax/eq, and 1.095 Å in 7-eq/eq (Table 5). In terms of calculated one-bond coupling constants, no Perlin effect is found in 7-ax/ax ($^1J_{C(5)-H_{ax}} \cong ^1J_{C(5)-H_{eq}}$), whereas “reverse” Perlin effects are seen in 7-ax/eq and 7-eq/eq. This observation might be more in line with interpretation in terms of $\sigma_{C-N} \rightarrow \sigma^*_{C-H_{eq}}$ hyperconjugative interactions.

Conclusions

Density functional calculations of the NMR $^1J_{C-H}$ coupling constants of a series of 1,3-diheterocyclohexanes are presented.

It is shown that even though the coupling constants depend on geometry, the sign of the difference between $J_{C-H_{ax}}$ and $J_{C-H_{eq}}$ is preserved. This allows one to be confident of the nature of the Perlin effect predicted with density functional theory (DFT) optimized geometries. After the theoretical confidence ranges (≈ 3 Hz) are considered, DFT-NMR, as developed by Malkin, Malkina, and Salahub, is a very important tool for the correct assignment of the direction of Perlin effects in 1,3-diheterocyclohexanes.

It is shown that for these systems, there is no correlation between the $^1J_{C-H}$ coupling constants and the corresponding C—H bond distances.

The results presented in this work indicate that the calculated one-bond coupling constants subjected to stereoelectronic effects deviate more from the experimental values than those that are not affected by these interactions. More precise determinations will require the consideration of solvent and thermal effects on coupling constants. We are presently examining such effects.

Acknowledgment. We gratefully acknowledge Prof. D. R. Salahub for his comments and M. Kuthy for a revision of this manuscript. We are grateful to the Dirección General de Servicios de Cómputo Académico, Universidad Nacional Autónoma de México, DGSCA, UNAM, for computational support and the generous gift of supercomputer time on a Cray Y-MP4/464, to Consejo Nacional de Ciencia y Tecnología (CONACYT) for financial support via grants 3279P-E9607 and L-0006E-E9607, and to Dirección General de Asuntos del Personal Académico (DGAPA) via grant IN107597.

References and Notes

- (1) Instituto de Química, UNAM.
- (2) Instituto Politécnico Nacional.
- (3) Universidad Autónoma Metropolitana-Iztapalapa.
- (4) Bohlmann, F. *Angew. Chem.* **1957**, 69, 641. Bohlmann, F. *Chem. Ber.* **1958**, 91, 2157.
- (5) (a) Krueger, P. J.; Jan, J.; Wieser, H. *J. Mol. Struct.* **1970**, 5, 375. (b) Bernardi, F.; Schlegel, H. B.; Wolfe, S. *J. Mol. Struct.* **1976**, 35, 149. (c) McKean, D. C. *Chem. Soc. Rev.* **1978**, 7, 399. (d) Hehre, W. J.; Radom, L.; Schleyer, P. v. R.; Pople, J. A. *Ab Initio Molecular Orbital Theory*; Wiley: New York, 1986.
- (6) Perlin, A. S.; Casu, B. *Tetrahedron Lett.* **1969**, 2921.
- (7) (a) Bock, K.; Wiebe, L. *Acta Chem. Scand.* **1973**, 27, 2676. See also: (b) Rao, V. S.; *Can. J. Chem.* **1982**, 60, 1067. (c) Hansen, P. E. *Prog. Nucl. Magn. Reson. Spectrosc.* **1981**, 14, 175.
- (8) Bailey, W. F.; Rivera, A. D.; Rossi, K. *Tetrahedron Lett.* **1988**, 29, 5621.
- (9) (a) Wolfe, S.; Pinto, B. M.; Varma, V.; Leung, R. Y. N. *Can. J. Chem.* **1990**, 69, 1051. (b) Wolfe, S.; Kim, C.-K. *Can. J. Chem.* **1991**, 69, 1408.
- (10) (a) Juaristi, E.; Cuevas, G. *Tetrahedron Lett.* **1992**, 33, 1847. (b) Juaristi, E.; Cuevas, G.; Flores-Vela, A. *Tetrahedron Lett.* **1992**, 33, 6927.
- (11) Juaristi, E.; Cuevas, G.; Vela, A. *J. Am. Chem. Soc.* **1994**, 116, 5796.
- (12) Eliel, E. L.; Rao, V. S.; Vierhapper, F. W.; Juaristi, G. Z. *Tetrahedron Lett.* **1975**, 4339.
- (13) Cuevas, G.; Juaristi, E.; Vela, A. *J. Mol. Struct. (THEOCHEM)* **1997**, 418, 231.

- (14) (a) Malkin, V. G.; Malkina, O. L.; Casida, M. E.; Salahub, D. R. *J. Am. Chem. Soc.* **1994**, *116*, 5898. (b) Malkin, V. G.; Malkina, O. L.; Eriksson, L. A.; Salahub, D. R. In *Modern Density Functional Theory. A Tool for Chemistry*; Seminario, J. M., Politzer, P., Eds.; Elsevier: Amsterdam, 1995.
- (15) Kowalewski, J. *Prog. NMR Spectrosc.* **1977**, *11*, 1. Kowalewski, J. *Ann. Rep. NMR Spectrosc.* **1982**, *12*, 81. Fukui, H. *Nucl. Magn. Reson.* **1991**, *20*, 107. Fukui, H. *Nucl. Magn. Reson.*, **1993**, *22*, 138. Oddershede, J. *Nucl. Magn. Reson.* **1992**, *21*, 113. Peruchena, N. M.; Contreras, R. H. *J. Mol. Struct. (THEOCHEM)* **1995**, *338*, 25.
- (16) Becke, A. D. *Can. J. Chem.* **1988**, *88*, 1052. Becke, A. D. *Phys. Rev. A* **1988**, *38*, 3098.
- (17) Perdew, J. P. *Phys. Rev. Lett.* **1985**, *55*, 1665.
- (18) Cf.: Andzelm, J.; Wimmer, E. *J. Chem. Phys.* **1992**, *96*, 1280. Andzel, J. In *Density Functional Methods in Chemistry*; Labanowski, J., Ed.; Springer: New York, 1991; p 155.
- (19) Frisch, M. J.; Trucks, G. W.; Schlegel, H. B.; Gill, P. M. W.; Johnson, B. G.; Wong, M. W.; Foresman, J. B.; Robb, M. A.; Head-Gordon, M.; Replogle, E. S.; Gomperts, R.; Andres, J. L.; Raghavachari, K.; Binkley, J. S.; Gonzalez, C.; Martin, R. L.; Fox, D. J.; Defrees, D. J.; Baker, J.; Stewart, J. J. P.; Pople, J. A. Gaussian 92/DFT, Revision G; Gaussian, Inc.: Pittsburgh, PA, 1993.
- (20) Stephens, P. J.; Devlin, F. J.; Chabalowski, C. F.; Frisch, M. J. *J. Phys. Chem.* **1994**, *98*, 11623. Becke, A. D. *J. Chem. Phys.* **1993**, *98*, 1372, 5648.
- (21) Lee, C.; Yang, W.; Parr, R. G. *Phys. Rev.* **1988**, *B37*, 785–789. Miehlich, B.; Savin, A.; Stoll, H.; Preuss, H. *Chem. Phys. Lett.* **1989**, *157*, 200.
- (22) Vosko, S. H.; Wilk, L.; Nusair, M. *Can. J. Phys.* **1980**, *58*, 1200.
- (23) Malkin, V. G.; Malkina, O. L.; Salahub, D. R. *Chem. Phys. Lett.* **1994**, *221*, 91.
- (24) Malkina, O. L.; Salahub, D. R.; Malkin, V. G. *J. Chem. Phys.* **1996**, *105*, 8793.
- (25) Salahub, D. R.; Fournier, R.; Mlynarski, P.; Papai, I.; St-Amant, A.; Uskio, J. In *Density Functional Methods in Chemistry*; Labanowski, J. K., Andzelm, J. W., Eds.; Springer: New York, 1991; p 77.
- (26) St-Amant, A.; Salahub, D. R. *Chem. Phys. Lett.* **1990**, *169*, 387.
- (27) Perdew, J. P.; Wang, Y. *Phys. Rev. B* **1986**, *33*, 8800.
- (28) Perdew, J. P. *Phys. Rev. B* **1986**, *33*, 8822; **1986**, *34*, 7406.
- (29) Kutzelnigg, W.; Fleischer, U.; Schindler, M. In *NMR—Basic Principles and Progress*; Springer-Verlag: Heidelberg, **1990**; Vol. 33, p 165.
- (30) Glendening, E. D.; Reed, A. E.; Carpenter, J. E.; Weinhold, F.; NBO 3.1; Theoretical Chemistry Institute, University of Wisconsin: Madison, WI, 1994. Reed, E. A.; Weinstock, R. B.; Weinhold, F. J. *J. Chem. Phys.* **1985**, *83*, 735. Reed, E. A.; Weinhold, F. J. *J. Chem. Phys.* **1985**, *83*, 1736. Reed, E. A.; Curtiss, L. A.; Weinhold, F. *Chem. Rev.* **1988**, *83*, 735.
- (31) Chertkov, V. A.; Sergeyev, N. M. *J. Am. Chem. Soc.* **1977**, *99*, 6750.
- (32) (a) Anderson, J. E.; Bloodworth, A. J.; Cai, J.; Davies, A. G.; Tallant, N. A. *J. Chem. Soc., Chem. Commun.* **1992**, 1689. (b) Anderson, J. E.; Bloodworth, A. J.; Cai, J.; Davies, A. G.; Schiesser, C. H. *J. Chem. Soc., Perkin Trans. 2* **1993**, 601.
- (33) (a) Anet, F. A. L.; Kopelevich, M. *J. Am. Chem. Soc.* **1986**, *108*, 2109. (b) Anet, F. A. L.; Kopelevich, M. *J. Chem. Soc., Chem. Commun.* **1987**, 595. (c) Forsyth, D. A.; Hanley, J. A. *J. Am. Chem. Soc.* **1987**, *109*, 7930.
- (34) Anderson, J. E.; Cai, J.; Davies, A. G. *J. Chem. Soc., Perkin Trans. 2* **1997**, 2633. We are grateful to Professor Davies for providing us with a copy of this manuscript prior to publication.